



**HAL**  
open science

# Effect of acidic components (SO<sub>4</sub><sup>2-</sup> and WO<sub>3</sub>) on the surface acidity, redox ability and NH<sub>3</sub>-SCR activity of new CeO<sub>2</sub>-TiO<sub>2</sub> nanoporous aerogel catalysts: A comparative study

Jihene Arfaoui, Abdelhamid Ghorbel, Carolina Petitto, Gérard Delahay

## ► To cite this version:

Jihene Arfaoui, Abdelhamid Ghorbel, Carolina Petitto, Gérard Delahay. Effect of acidic components (SO<sub>4</sub><sup>2-</sup> and WO<sub>3</sub>) on the surface acidity, redox ability and NH<sub>3</sub>-SCR activity of new CeO<sub>2</sub>-TiO<sub>2</sub> nanoporous aerogel catalysts: A comparative study. *Inorganic Chemistry Communications*, 2022, 140, pp.109494. 10.1016/j.inoche.2022.109494 . hal-03648994

**HAL Id: hal-03648994**

**<https://hal.science/hal-03648994>**

Submitted on 22 Apr 2022

**HAL** is a multi-disciplinary open access archive for the deposit and dissemination of scientific research documents, whether they are published or not. The documents may come from teaching and research institutions in France or abroad, or from public or private research centers.

L'archive ouverte pluridisciplinaire **HAL**, est destinée au dépôt et à la diffusion de documents scientifiques de niveau recherche, publiés ou non, émanant des établissements d'enseignement et de recherche français ou étrangers, des laboratoires publics ou privés.

**Effect of acidic components (SO<sub>4</sub><sup>2-</sup> and WO<sub>3</sub>) on the surface acidity, redox ability and NH<sub>3</sub>-SCR activity of new CeO<sub>2</sub>-TiO<sub>2</sub> nanoporous aerogel catalysts: A comparative study**

Jihene Arfaoui<sup>\*a</sup>, Abdelhamid Ghorbel<sup>a</sup>, Carolina Petitto<sup>b</sup>, Gerard Delahay<sup>b</sup>

<sup>a</sup>Université Tunis El Manar, Laboratoire de Chimie des Matériaux et Catalyse, Département de Chimie, Faculté des Sciences de Tunis, Campus Universitaire Farhat Hached d'El Manar, 2092, Tunis, Tunisia.

<sup>b</sup>ICGM, Univ Montpellier, ENSCM (MACS), CNRS, Montpellier, France

\* Corresponding author: E-mail address: [jihene.arfaoui@fst.utm.tn](mailto:jihene.arfaoui@fst.utm.tn); [jihenar@yahoo.fr](mailto:jihenar@yahoo.fr)

Tel: +216 23020273, Fax: +216 71 875 008

**Abstract**

Selective catalytic reduction (SCR) of nitrogen oxide (NO) by ammonia (NH<sub>3</sub>) was studied in this work over new sulfate (SO<sub>4</sub><sup>2-</sup>) or tungsta (WO<sub>3</sub>) modified CeO<sub>2</sub>-TiO<sub>2</sub> aerogel catalysts. The catalytic systems were elaborated via sol gel method then characterized by: XRD, N<sub>2</sub>-Physisorption at 77 K, DRUV-vis, NH<sub>3</sub>-TPD and H<sub>2</sub>-TPR. It was revealed that the nature of acidic components influences differently the texture, surface oxygen concentration, acidity, reducibility and NH<sub>3</sub>-SCR activity of new Ce-based catalysts. Hence, the incorporation of sulfate modifies the nature of Ce species, improves their dispersion through the Ce-SO<sub>4</sub><sup>2-</sup> interactions and, particularly, generates new strong acid sites which display superior catalytic performance at high temperature NO reduction (NO conversion into N<sub>2</sub> > 90 % between 450 and 500 °C over CeO<sub>2</sub>-TiO<sub>2</sub>-SO<sub>4</sub><sup>2-</sup> catalyst). However, the addition of tungsta affects slightly the surface acidity of CeO<sub>2</sub>-TiO<sub>2</sub> catalyst but it induces the creation of more reactive surface oxygen and new redox sites at its surface (mainly due to the existence of W-Ce interactions) leading to highly active WO<sub>3</sub>-CeO<sub>2</sub>-TiO<sub>2</sub> system for the low temperature NH<sub>3</sub>-SCR reaction with above 90 % NO conversion into N<sub>2</sub> between 320 and 400 °C.

**Key words:** NO Emissions control, Modified CeO<sub>2</sub>-TiO<sub>2</sub> aerogel catalysts, Acidic components, Surface acidity, Redox ability, NH<sub>3</sub>-SCR activity.

## I. Introduction

Diesel engines are considered as one of the largest contributors to the environmental pollution and climate change caused by exhaust emissions containing hydrocarbons (HC), particulate matter (PM) carbon monoxide (CO) and nitrogen oxides (NO<sub>x</sub>). NO<sub>x</sub> (x = 1 and 2) are constituted by 85-95 % of NO which is an odorless and colorless gas and that is gradually converted, in atmospheric air, into NO<sub>2</sub> (a reddish brown gas with pungent odor and a level of toxicity five times greater than that of NO) [1]. These toxic compounds react chemically with other pollutants to form tropospheric ozone (the primary component of photochemical smog) and contribute to the formation of acid rain, haze, greenhouse gas... [1-4]. In addition, NO<sub>x</sub> species are harmful to the human body, causing eye and throat irritation, chest tightness, nausea, headache, lung infections and respiratory allergies like bronchitis and pneumonia [2,5].

In recent years, strict legislations and policies have been imposed worldwide for the purpose of reducing NO<sub>x</sub> emissions from vehicles. In Euro V, NO<sub>x</sub> emission is limited to <180 mg/km and 60 mg/km for diesel-driven engines and petrol-driven engines, respectively. These values are 55 % lower in Euro VI [2,6]. Besides, in China, the limits of NO<sub>x</sub> from light-duty vehicles are fixed at 60 mg/km and 35 mg/km (GB 18352.6-2016) for 2020 and 2023 years, respectively [7]. Consequently, the NO<sub>x</sub> removal from flue gases has become an ever more urgent task for environmental protection.

The NO<sub>x</sub> control technologies can be classified into three groups: combustion, pre-combustion, and post-combustion. In pre-combustion process, the formation of NO<sub>x</sub> is inhibited by the selection of a low-nitrogen fuel. Also, combustion is mainly used to reduce the NO<sub>x</sub> emissions by varying the combustion conditions. Nevertheless, using the post combustion methods, the NO<sub>x</sub> existing in the flue gas exhaust are converted into essentially

nitrogen ( $N_2$ ) and other harmless products via physical and chemical transformations which are produced in the denitrification devices installation [8]. Compared with pre-combustion and combustion methods (which help to remove less than 50 %  $NO_x$ ), the post-combustion technologies are more attractive due to its higher  $NO_x$  elimination (> 80 %) [2].

Among several available post-combustion technologies, including selective catalytic reduction (SCR), selective non catalytic reduction (SNCR), electrochemical reduction, catalytic decomposition, non-thermal plasma (NTP), wet scrubbing, adsorption and electron beam [2,8,10] SCR of  $NO_x$  with  $NH_3$ , is currently the most popular approach for flue gases denitrification (De $NO_x$ ) from stationary and mobile sources [10,11] ; it is based on the reaction between  $NO_x$  and  $NH_3$  to produce  $N_2$  and  $H_2O$  using a suitable catalyst.  $V_2O_5$ - $WO_3/TiO_2$  system is the most widely used  $NH_3$ -SCR catalyst to abate  $NO_x$  from power plants. It was introduced also on diesel vehicles as the first generation of SCR catalyst [12, 13]. Nevertheless, this system still has some intrinsic drawbacks such as: the narrow and high working temperature window (300-400 °C), low  $N_2$  selectivity at high-temperature and toxicity of vanadium [14, 15]. Accordingly, many research works have been realized to develop vanadium-free catalysts that can be applied to diesel vehicles [4].

It is recognized that the presence of actives acidic and redox sites on the catalyst surface is a key factor for the design of SCR catalysts with a high  $NO_x$  removal efficiency [16-19]. Recently, a lot of attention have been devoted to  $CeO_2$ - $TiO_2$  systems as great candidate to substitute the commercial  $VO_x$ - $TiO_2$  catalysts due to their environmentally friendly and excellent SCR performance. A detailed review about the investigations of  $CeO_2$ - $TiO_2$  catalysts in the  $NH_3$ -SCR reaction was recently reported by Zheng et al. [16]. The studies demonstrated that  $CeO_2$ - $TiO_2$  catalysts, prepared via different methods (Impregnation, co-precipitation, homogenous precipitation, spontaneous deposition, sol gel (xerogel form), co-precipitation associated with microwave, supercritical water and dry ball milling in the

presence of an organic ligand), have been proved to be very active in the reduction of NO by NH<sub>3</sub> due to the unique oxygen storage capacity (OSC) of cerium, its excellent redox ability and acid base properties [16,20, 21]. In this framework, Gao et al. [22,23] reported that CeO<sub>2</sub>-TiO<sub>2</sub> xerogel catalyst, elaborated via sol-gel method, exhibits much better NH<sub>3</sub>-SCR performance than the same catalysts prepared by impregnation and co-precipitation methods, owing to its high surface area, better redox ability, strong interaction between CeO<sub>2</sub> and TiO<sub>2</sub> and well dispersed CeO<sub>2</sub> species. On the other hand, many literature reports have proved that adding acidic components (sulfuric acid [24], phosphoric acid [25]; oxides of: W [26], Mo [27] or Nb [28]) into Ce based catalysts enhances its acidic functions and thereby improves significantly its NO-NO-SCR activity. Yu et al. [29], investigated a series of sulfated catalysts (CuSO<sub>4</sub>/TiO<sub>2</sub>, Fe<sub>2</sub>(SO<sub>4</sub>)<sub>3</sub>/TiO<sub>2</sub>, MnSO<sub>4</sub>/TiO<sub>2</sub>, Ce(SO<sub>4</sub>)<sub>2</sub>/TiO<sub>2</sub> and CoSO<sub>4</sub>/TiO<sub>2</sub>) in the NH<sub>3</sub>-SCR reaction and demonstrated that the amount of acid sites was the main factor which affects the catalytic activity of metal sulfate catalysts. Furthermore, in our previous work [26], we showed that WO<sub>3</sub>-CeO<sub>2</sub>-TiO<sub>2</sub> exhibits higher SCR activity than WO<sub>3</sub>-TiO<sub>2</sub> and CeO<sub>2</sub>-TiO<sub>2</sub> aerogel catalysts due to the synergetic effect between W and Ce which influences the acidity and reducibility of catalyst. Li et al. [30] reported that a novel CeO<sub>2</sub>/TiO<sub>2</sub>-MoO<sub>3</sub> catalyst exhibits 100% NO conversion at 200-350 °C. The authors indicated that doping of Mo produces more Brønsted acid and Lewis acid sites, increases the specific surface area and redox ability of catalyst and, consequently, enhances its NH<sub>3</sub>-SCR activity. A series of CeO<sub>2</sub>-Nb<sub>2</sub>O<sub>5</sub>/TiO<sub>2</sub> SCR catalysts were investigated by Jiang et al. [28]. Their results revealed that the addition of Nb improves the dispersion of CeO<sub>2</sub>, increases the amount of Ce<sup>3+</sup> and chemisorbed oxygen species on the catalyst surface, which enhances the catalytic activity of CeTi material. The authors attributed the superior SCR activity of CeNbTi to its high redox ability, the enhanced adsorption capacity of NH<sub>3</sub> species and the synergistic action between Ce, Nb and Ti species.

Although CeO<sub>2</sub>-TiO<sub>2</sub> catalysts have been extensively studied and demonstrated a high catalytic performance in the NH<sub>3</sub>-SCR reaction, the investigation of the aerogel form of CeO<sub>2</sub>-TiO<sub>2</sub> in this reaction is still rare and only a few paper deal with this subject. Therefore, in this study we report for the first time a comparative investigation about the effect of acidic components (SO<sub>4</sub><sup>2-</sup> or WO<sub>3</sub>) on the physicochemical properties and NH<sub>3</sub>-SCR activity of Ce based aerogel catalysts (CeO<sub>2</sub>-TiO<sub>2</sub>-SO<sub>4</sub><sup>2-</sup> and WO<sub>3</sub>-CeO<sub>2</sub>-TiO<sub>2</sub>). These materials were elaborated via sol gel procedure followed by supercritical drying. This method presents several advantages including a simple and low cost technology, low process-temperatures and flexible control of the structure and size of final products using many operating parameters [31]. In addition, it can give aerogel mixed oxides with interesting properties, such as: high purity, nanometer size and developed mesoporous texture..., which make them useful for many applications, especially for catalysis [20, 26, 32].

## **2. Material and methods**

### *2. 1. Synthesis of Ce based nanoporous aerogel catalysts*

The powder aerogels (TiO<sub>2</sub>, CeO<sub>2</sub>-TiO<sub>2</sub>, CeO<sub>2</sub>-TiO<sub>2</sub>-SO<sub>4</sub><sup>2-</sup> and WO<sub>3</sub>-CeO<sub>2</sub>-TiO<sub>2</sub>) were prepared via the one step sol gel protocol, then dried under the supercritical drying conditions of solvent (ethanol). The detailed method adopted for the elaboration of samples was described in our previous works [20,26]. Ammonium metatungstate hydrate ((NH<sub>4</sub>)<sub>6</sub>H<sub>2</sub>W<sub>12</sub>O<sub>24</sub>.xH<sub>2</sub>O, Sigma Aldrich, > 99.9%) and cerium nitrate (Ce(NO<sub>3</sub>)<sub>3</sub>.6H<sub>2</sub>O, Aldrich) were used as W and Ce precursors, respectively. Theoretical loading of WO<sub>3</sub> or CeO<sub>2</sub> were fixed at 10 % wt. For the sulfated catalyst, an appropriate volume of H<sub>2</sub>SO<sub>4</sub> solution (Scarlau, 95-97%) giving a molar ratio S/Ti = 0.2 was used. All the aerogel mixed oxides were calcined at 500 °C for 3 h under O<sub>2</sub> flow (30 mL.min<sup>-1</sup>).

## 2. 2. Characterization of Ce based nanoporous aerogel catalysts

The structure and crystallites size of aerogels (powder) were determined by X Ray Diffraction (XRD) analysis using a Brüker AXS D8 diffractometer. The XRD patterns were registered, between 2 and 80 ° with CuK $\alpha$  radiation ( $\lambda = 1.5406 \text{ \AA}$ ). The main reflexion of TiO<sub>2</sub> anatase phase ( $\sim 2\theta = 25 \text{ }^\circ$ , hkl: 101), was used to determine the crystallites size (D) of solids based on the Scherrer formula ( $D = 0.89 (\lambda / \beta \cos\theta)$ ) [33] where  $\lambda$  is the wavelength of XR radiation,  $\beta$  is the corrected peak width at half-maximum intensity (FWHM in radians), and  $\theta$  is the 101 reflection position.

The textural properties of solids were examined by the N<sub>2</sub> physisorption at 77 K. N<sub>2</sub> adsorption-desorption isotherms, specific surface area ( $S_{\text{BET}}$ ), total pore volume ( $V_{\text{PT}}$ ), pore size distribution and pore size diameter ( $\Phi_{\text{pore}}$ ) were determined by means of a Micromeritics ASAP 2020 apparatus. The powder was outgassed in a vacuum during 6 h at 200 °C prior to N<sub>2</sub> adsorption. The residual pressure reached during the degassing step was 10<sup>-5</sup> Torr.

The UV-vis analyses were carried out on a PerkinElmer spectrophotometer type lambda 45 equipped with an integrating sphere type RSA-PE-20. The UV-vis spectra were recorded at room temperature in the 200-900 nm range.

The NH<sub>3</sub> temperature-programmed desorption (NH<sub>3</sub>-TPD) experiments were performed using an AUTOCHEM 2920 (Micromeritics) equipped with a TCD detector. For the analysis, 0.05 g of each sample was pretreated in air flow (30 mL min<sup>-1</sup>) at 500 °C (ramp 10 °C min<sup>-1</sup>) for 30 min, then cooled to 100 °C in the same stream and subsequently exposed to NH<sub>3</sub> (5 vol% NH<sub>3</sub> in He, flow rate = 30 mL min<sup>-1</sup>) for 45 min. The physisorbed NH<sub>3</sub> was removed by flushing the catalyst with He (30 mL min<sup>-1</sup>) for 2 h. Finally, the NH<sub>3</sub>-TPD curves

were recorded by heating the samples in He (30 mL min<sup>-1</sup>) at a heating rate of 10 °C min<sup>-1</sup> from 100 to 600 °C.

The H<sub>2</sub> temperature-programmed reduction (H<sub>2</sub>-TPR) analyses were done in an AUTOCHEM 2910 (Micromeritics) over 0.05 g of sample. The H<sub>2</sub> consumption was measured by a thermal conductivity detector. First, the sample was pretreated at 500 °C with 5 vol % O<sub>2</sub> in He (30 mL min<sup>-1</sup>) for 30 min (ramp 10 °C min<sup>-1</sup>). After being cooled down to 50 °C in the same atmosphere, the sample was flushed with He (30 mL min<sup>-1</sup>), then exposed to a flow containing 5 vol % H<sub>2</sub> in Ar (30 mL min<sup>-1</sup>) and heated from 50 to 800 (or 900 °C) at a heating rate of 10 °C min<sup>-1</sup>.

### *2. 3. Catalytic activity measurement*

The selective Catalytic Reduction (SCR) tests were carried out in a fixed-bed quartz flow reactor, operating at atmospheric pressure. Before measurements, the catalyst (0.05 g) was activated in situ at 200 °C for 30 min under O<sub>2</sub>/He (20/80, v/v) flow then cooled to 100 °C. Afterward, the NO conversion curves were recorded between 100 and 500 °C with the heating rate of 6 °C min<sup>-1</sup>. The reaction conditions are: 400 ppm NO, 400 ppm NH<sub>3</sub>, 8 % O<sub>2</sub> in He and 100 mL min<sup>-1</sup> total flow rate yielding a gas hourly space velocity (GHSV) of 120,000 h<sup>-1</sup>. During the SCR test, the reactants and products gases were continuously analyzed by an online Pfeiffer Omnistar quadruple mass gas spectrometer equipped with Channeltron and Faraday detectors (0-200 amu).

## **3. Results and discussion**

### *3. 1. Physico-chemical properties of Ce based nanoporous aerogel catalysts*

The XRD patterns of powder aerogels and average crystallites size of TiO<sub>2</sub> carrier are given in Fig. 1 and Table 1, respectively. The peaks, detected at  $2\theta \approx 25.3^\circ$  (hkl:101);  $36.9^\circ$ (103);  $37.8^\circ$  (004);  $38.6^\circ$  (112);  $48.2^\circ$  (200);  $53.9^\circ$  (105);  $55.2^\circ$  (211);  $62.7^\circ$  (204);  $69.0^\circ$

(116);  $70.4^\circ$  (220) and  $75.2^\circ$  (215) [ICSD 01-083-2243], in the diffractograms of all the solids are consistent with the characteristic reflections of  $\text{TiO}_2$  anatase phase. There are no peaks related to rutile or brookite phases revealing the synthesis of  $\text{TiO}_2$  carrier with a high purity of anatase form. Generally, the catalytic activity of SCR catalysts with anatase  $\text{TiO}_2$  as carrier was superior to that with rutile or brookite  $\text{TiO}_2$  as catalytic support [12, 17]. On the other hand, no typical peaks of tungsten oxide or metal sulfates were observed in the obtained XRD diffraction patterns indicating that tungsten and sulfates species are highly dispersed at  $\text{TiO}_2$  surface. This is in agreement with the results already obtained for numerous  $\text{WO}_3$  containing catalysts [26,34] such as: xerogel  $\text{WO}_3\text{-CeO}_2\text{-TiO}_2$  [35] and supported metal sulfates on  $\text{Ce-TiO}_x$  SCR catalysts [36]. In the case of unsulfated catalysts, the new peaks of low intensity, located at  $2\theta \approx 28.5^\circ$  (hkl: 111) and  $32.9^\circ$  (200), are attributed to a low amount of the crystalline form of cubic ceria ( $\text{CeO}_2$ ) [ICSD 00-034-0394]. These peaks are absent in the diffractogram of  $\text{CeO}_2\text{-TiO}_2\text{-SO}_4^{2-}$  catalyst indicating the highly dispersed state of cerium species at the surface of sulfated catalyst. This is mainly due to the existence of strong interactions between Ce and  $\text{SO}_4^{2-}$ .

From the values listed in table 1, it can be concluded that all the powder aerogels are constituted by nano-sized particles with a size in the range of  $\sim 8\text{-}11$  nm. It could be also mentioned that, contrarily to sulfate groups, the presence of W species inhibits the crystallites growth of anatase  $\text{TiO}_2$ , since a visible increase of  $\text{TiO}_2$  grain is noted for the sulfated sample only. Shan et al. [37] indicated that the Ce species inhibited also the growth of anatase  $\text{TiO}_2$  crystallite in the case of  $\text{CeO}_2\text{-TiO}_2$  catalyst, prepared via an optimized homogeneous precipitation method.

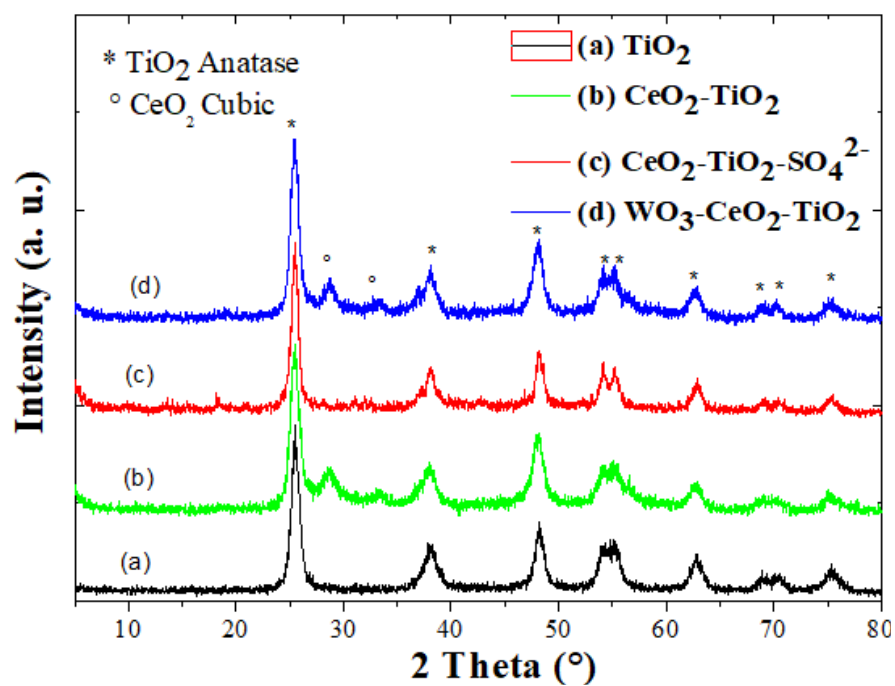


**Figure 1.** Structure of Ce based nanoporous aerogel catalysts.

**Table 1.** Crystalline phases and TiO<sub>2</sub> crystallites size of Ce based nanoporous aerogel catalysts.

Sample	XRD phases	FWHM (°)	TiO <sub>2</sub> crystallites size D (nm)
TiO <sub>2</sub>	Anatase	0.892	8.6
CeO <sub>2</sub> -TiO <sub>2</sub>	Anatase + Ceria	0.884	8.6
TiO <sub>2</sub> -CeO <sub>2</sub> -SO <sub>4</sub> <sup>2-</sup>	Anatase	0.689	11.1
WO <sub>3</sub> -CeO <sub>2</sub> -TiO <sub>2</sub>	Anatase + Ceria	0.931	8.2

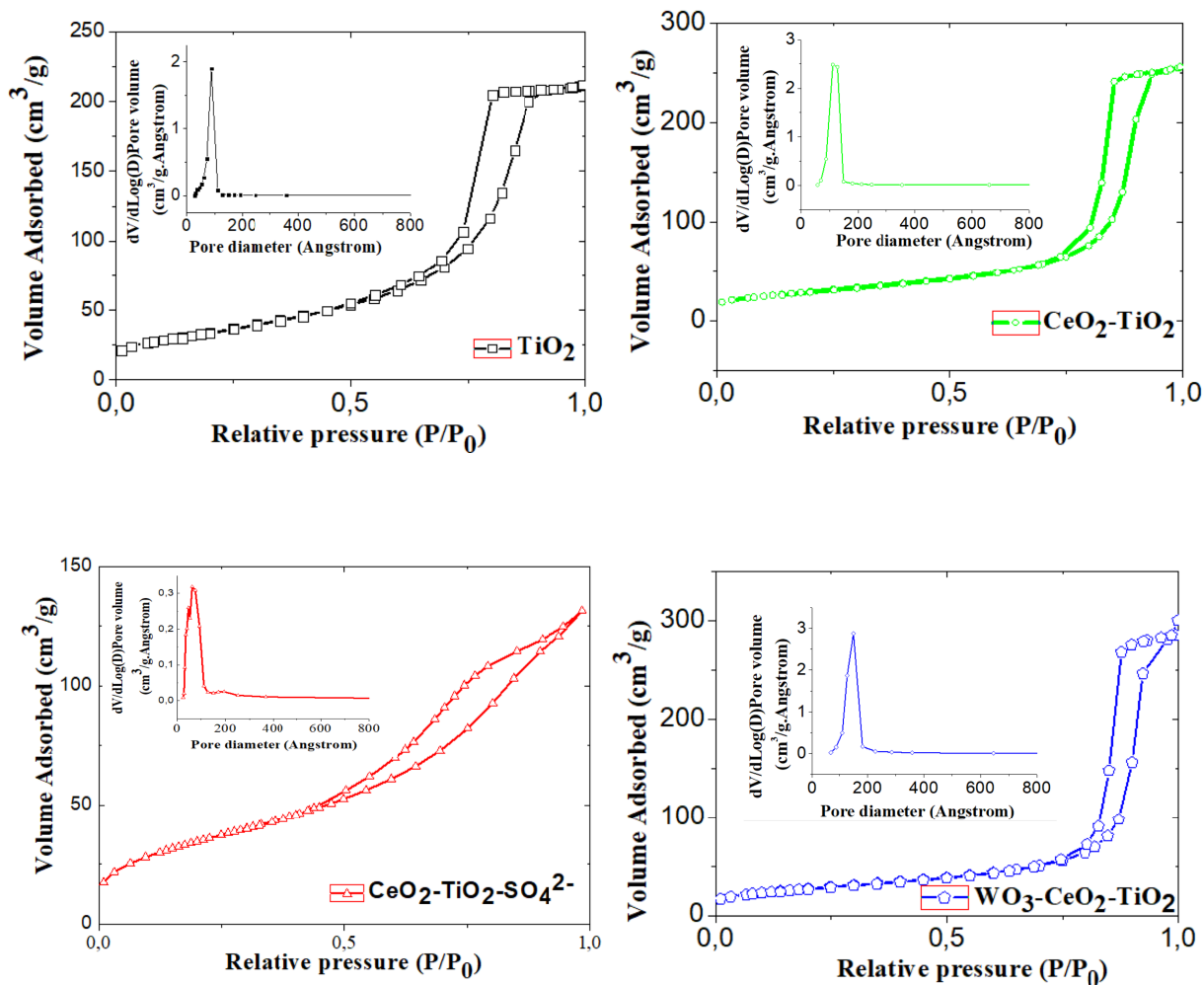


**Figure 2.** N<sub>2</sub>-Isotherms and corresponding pore size distribution curves of Ce based nanoporous aerogel catalysts.

N<sub>2</sub> adsorption-desorption isotherm and corresponding pore size distribution curve of each sample are depicted in Figure 2. As it can be seen, an isotherm belonging to type IV, is obtained for all the aerogels and is indicative, according to the IUPAC classification, of their mesoporous texture [38]. Pure TiO<sub>2</sub> and CeO<sub>2</sub>-TiO<sub>2</sub> exhibit a H2 type of hysteresis loops demonstrating the presence of ink-bottle pores in their texture [39]. However, cylindrical mesoporous channels exist in the texture of WO<sub>3</sub>-CeO<sub>2</sub>-TiO<sub>2</sub> system that is characterized by a H1 type of hysteresis loop [40]. For the sulfated catalyst (CeO<sub>2</sub>-TiO<sub>2</sub>-SO<sub>4</sub><sup>2-</sup>), the obtained hysteresis loop mostly resembles to H3 type related to mesoporous solids with a broad distribution of the pores size [29,41,42].

As indicated in Table 2, the high values of the specific surface area ( $S_{\text{BET}} > 99 \text{ m}^2/\text{g}$ ) and total pore volume ( $V_{\text{PT}} > 0.21 \text{ cm}^3/\text{g}$ ) obtained in all cases demonstrate that all the investigated catalysts develop a good mesoporous texture which is beneficial for their NO-SCR activity. Nevertheless, it should be mentioned that the slight decrease of the  $S_{\text{BET}}$  observed in the case of  $\text{CeO}_2\text{-TiO}_2$  and  $\text{WO}_3\text{-CeO}_2\text{-TiO}_2$  catalysts can be related to the blockage of some pores of  $\text{TiO}_2$  by Ce and/or W species [20]. Conversely, the high  $S_{\text{BET}}$  retained for the sulphated catalyst can be explained by the high dispersion of cerium species at the catalyst surface due to their interactions with sulfate groups. This is consistent with the obtained XRD results.

**Table 2.** Textural properties of Ce based nanoporous aerogels catalysts.

Sample	BET surface area ( $\text{m}^2/\text{g}$ )	Total pore volume ( $\text{cm}^3/\text{g}$ )	Average Pore diameter ( $\Phi_{\text{pore}}$ , Å)
$\text{TiO}_2$	122	0.33	79
$\text{CeO}_2\text{-TiO}_2$	106	0.40	117
$\text{TiO}_2\text{-CeO}_2\text{-SO}_4^{2-}$	128	0.21	62
$\text{WO}_3\text{-CeO}_2\text{-TiO}_2$	99	0.46	145

Fig. 3 shows the UV-vis spectra of powder aerogels. It is clearly seen that all the solids display the characteristics bands of  $\text{TiO}_2$  anatase phase located in the 200-400 nm range and attributed to  $\text{O}^{2-} \rightarrow \text{Ti}^{4+}$  charge transfer transitions [20,43]. Additional bands appeared above 350 nm in the UV spectra of  $\text{CeO}_2\text{-TiO}_2$  and  $\text{WO}_3\text{-CeO}_2\text{-TiO}_2$  catalysts and could be ascribed, based on the literature reports, to cerium and tungsten species;  $\text{Ce}^{4+}$  (280-400 nm [20, 26]) and  $\text{W}^{6+}$  polymeric octahedral species (300-375 nm [26, 34, 44]). Remarkable, the shape of the UV-vis curve of  $\text{CeO-TiO}_2$  is strongly changed after sulfate incorporation. In fact, we note the disappearance of bands related to  $\text{Ce}^{4+}$  species (in the 280-400 nm range [26, 34, 45, 46]), which implies that sulfate groups obviously affect the nature of cerium species (perhaps oxidation state, dispersion and/ or coordination). This suggests, in perfect agreement with our

previous work [20] and in line with the XRD results, the existence of strong interactions between Ce species and sulfate groups which, most probably, contribute to stabilize cerium at its  $Ce^{3+}$  form (characterized by  $O^{2-} \rightarrow Ce^{3+}$  absorption bands in the range of 220-250 nm) [20, 26, 47]. Similar observations demonstrating the modification of the nature of Mn species after sulfate addition have been previously stated for Mn based aerogel catalysts [47].

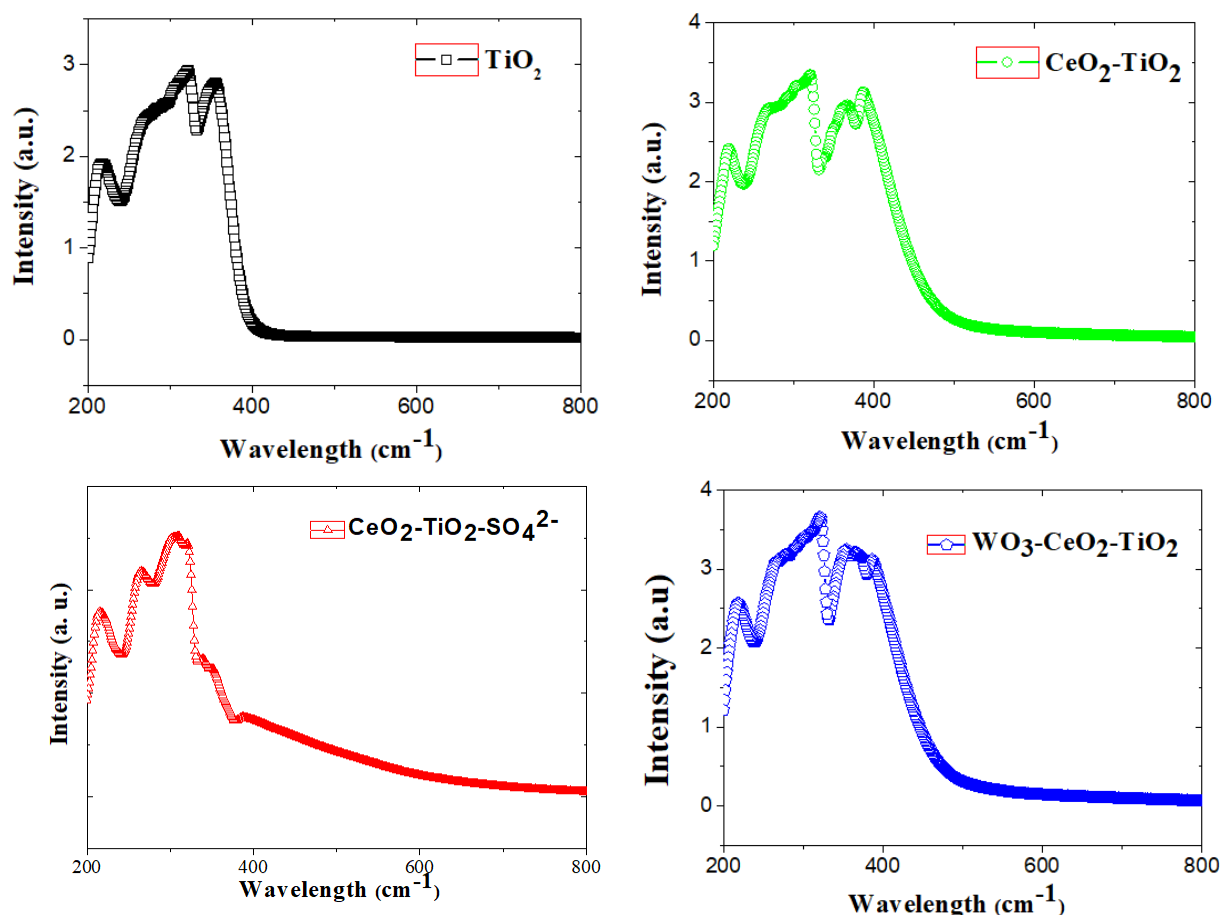


**Figure 3.** UV-vis spectra of Ce based nanoporous aerogel catalysts.

The  $NH_3$  adsorption on the acidic sites of catalyst is known to be a crucial step for NO-SCR reaction, especially over catalytic systems used under high temperature ( $> 300\text{ }^\circ\text{C}$ , [48,49]).  $NH_3$ -TPD experiments were performed in order to explore the surface acidity of aerogel catalysts and the results are illustrated in Fig. 4. As observed, all the samples display a broad  $NH_3$  desorption signal from 100 to 400  $^\circ\text{C}$  which could be assigned to ammonia

desorbed from weak and medium acid sites [50]. The shape and intensity of this signal changes as function of the nature of active element added to TiO<sub>2</sub> suggesting the existence of strong and diverse interactions between titania support and supported species (Ce, W, SO<sub>4</sub><sup>2-</sup>) which affect differently the number and strength of acid sites [44,47]. Remarkably a new high temperature NH<sub>3</sub> desorption peak centered at around 515 °C is detected in the NH<sub>3</sub>-TPD profile of sulphated sample only and is ascribed, according to our previous studies [20,41,47] to new strong acid sites generated by sulfate groups. Based on the above results, it can be concluded that adding WO<sub>3</sub> or SO<sub>4</sub><sup>2-</sup> influences differently the surface acidity of CeO<sub>2</sub>-TiO<sub>2</sub> catalyst and higher total acidity is obtained by adding sulfate groups.

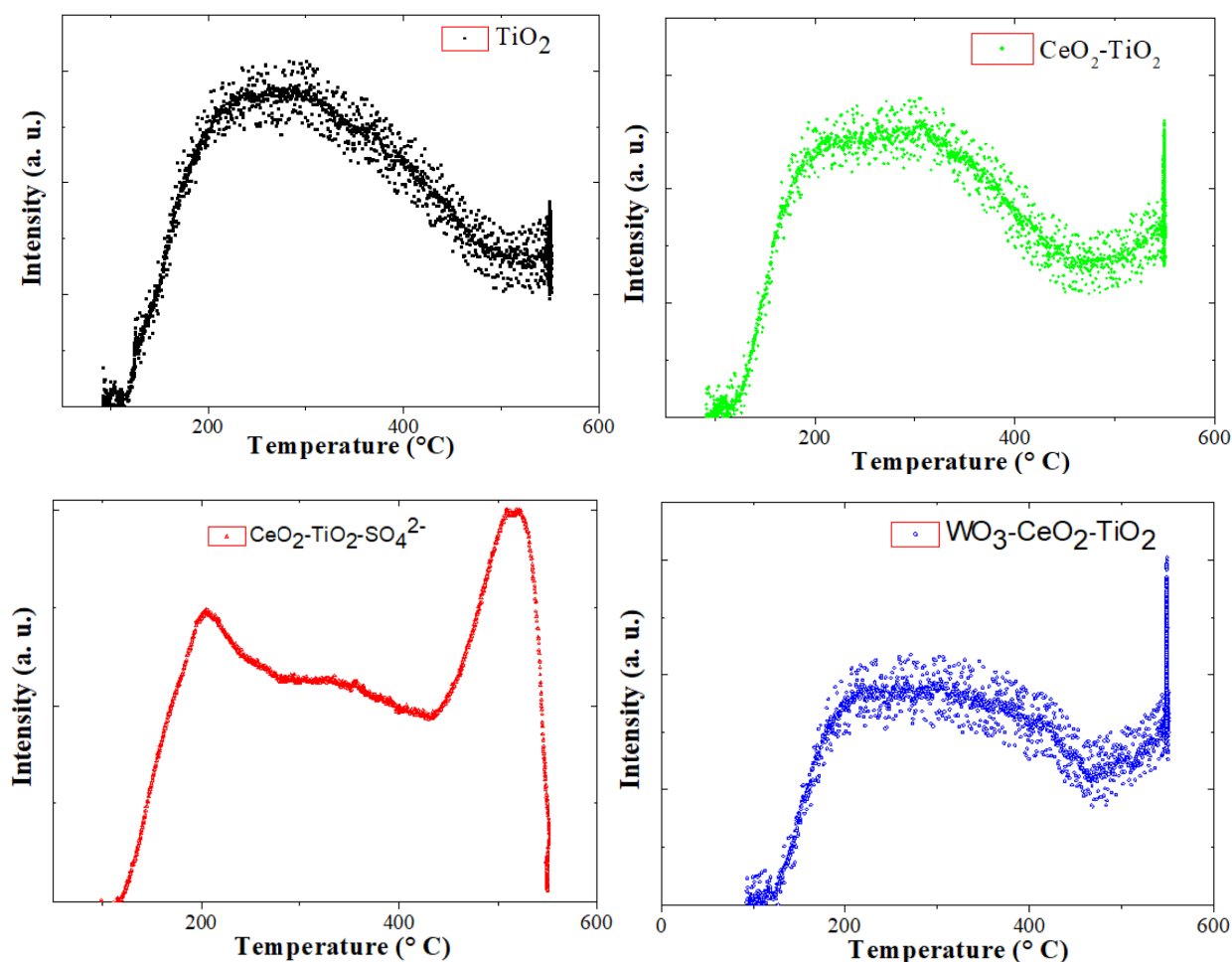


**Figure 4.** NH<sub>3</sub>-TPD curves of Ce based nanoporous aerogel catalysts.

The redox ability of catalyst plays a key role in the NH<sub>3</sub>-SCR reaction [51]. It was reported that the redox properties have a significant influence on the NH<sub>3</sub>-SCR performance

of CeO<sub>2</sub>-TiO<sub>2</sub> catalysts. Usually, a suitable redox property facilitates the activation of NO<sub>x</sub> and NH<sub>3</sub> at low temperature and thus increases the low temperature catalytic activity of CeO<sub>2</sub>-TiO<sub>2</sub> catalyst. Moreover, it is widely accepted that the adsorption and activation of oxygen and NO<sub>x</sub> occur at Ce<sup>4+</sup>/Ce<sup>3+</sup> redox sites [16]. The reducibility of CeO<sub>2</sub>-TiO<sub>2</sub> and the effects of adding sulfate and tungsta on the redox behaviour of this aerogel catalyst were examined by means of H<sub>2</sub>-TPR technique. The recorded H<sub>2</sub>-TPR curves are presented in Fig. 5. As shown, the incorporation of cerium contributes to the creation of redox sites at TiO<sub>2</sub> surface since the CeO<sub>2</sub>-TiO<sub>2</sub> sample displays H<sub>2</sub> consumption peaks in the 400 and 600 °C temperature range which can be attributed, according to literature reports, to the reduction of surface oxygen of stoichiometric ceria (Ce<sup>4+</sup>-O-Ce<sup>4+</sup>) and cerium species (Ce<sup>4+</sup> to Ce<sup>3+</sup>) [26,52]. The addition of acidic components (WO<sub>3</sub> or SO<sub>4</sub><sup>2-</sup>) influences in a different way the nature of redox sites and reducibility of CeO<sub>2</sub>-TiO<sub>2</sub> catalyst. Therefore, the WO<sub>3</sub>-CeO<sub>2</sub>-TiO<sub>2</sub> system demonstrates a broad first peak in the 300-500 °C temperature range corresponding to the reduction of surface oxygen of CeO<sub>2</sub> [26] and a second peak maximized at 570 °C attributed to the reduction of cerium species from Ce<sup>4+</sup> to Ce<sup>3+</sup> [20,26,52]. The intensities and areas of these peaks are higher compared to these obtained for CeO<sub>2</sub>-TiO<sub>2</sub> solid revealing the presence of higher quantities of surface oxygen and Ce redox sites at the WO<sub>3</sub>-CeO<sub>2</sub>-TiO<sub>2</sub> surface [26]. This is probably due to the existence of Ce-W interactions which enhance the redox ability of WCeTi catalyst. Noting also that WO<sub>3</sub>-CeO<sub>2</sub>-TiO<sub>2</sub> solid displays a third peak at 860 °C which is ascribed to the reduction of tungsten species [26,44]. The H<sub>2</sub>-TPR profile of sulfated catalyst is different from these registered for the other samples; it shows a new high intensive and asymmetrical peak beginning at around 450 °C and centered at ~ 650 °C which is ascribed to the reduction of sulfate groups [20,26,47]. For this sample, the reduction of surface oxygen of CeO<sub>2</sub> and cerium species seems to be overlapped by the former peak.

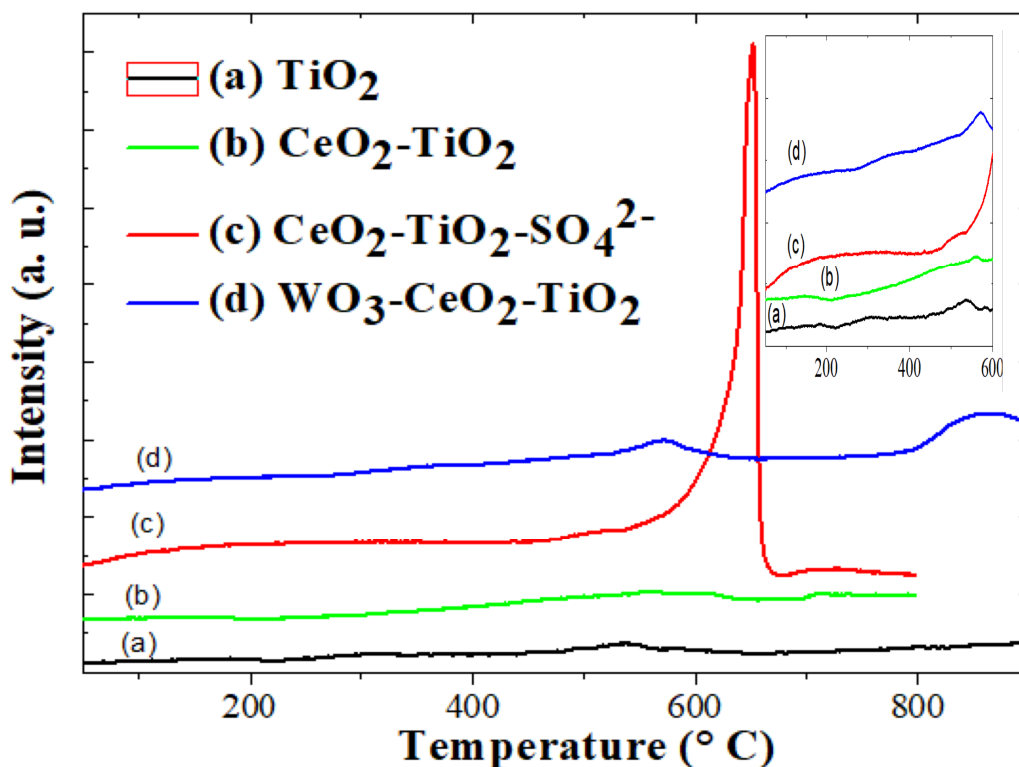


**Figure 5.** H<sub>2</sub>-TPR curves of Ce based nanoporous aerogel catalysts.

It was recognized that the SCR activity is governed by the reducibility of catalyst at low temperatures and by its acidity at high temperatures [53]. The NH<sub>3</sub>-SCR activity of Ce based aerogel catalysts was evaluated and the results, in term of NO conversion as function of reaction temperature, are illustrated in Fig 6A. Total conversion and oxidation conversion of NH<sub>3</sub> are also presented (Fig. 6B). As shown in Fig. 6A, the NO conversions are strongly dependent on the nature of active elements and reaction temperature. Therefore, the TiO<sub>2</sub> carrier is inactive at low temperatures (< 300 °C) and exhibits moderate reactivity at higher temperatures with a maximum of 50 % NO conversion into N<sub>2</sub> at 500 °C. The SCR activity is significantly enhanced at low temperatures after adding 10 wt. % CeO<sub>2</sub>. This increase in NO conversion is essentially attributed to the reactivity of cerium redox sites created at TiO<sub>2</sub> surface as demonstrated by the H<sub>2</sub>-TPR analysis. Noticeably, over this CeO<sub>2</sub>-TiO<sub>2</sub> aerogel catalyst, the NO conversion increases from 10 % (at 205 °C) to 90 % (at 330 °C) and remains above 90 % in the 330 - 400 °C interval. This high catalytic activity can be mainly correlated

with the presence of active surface oxygen and redox sites generated by the presence of cerium species at the  $\text{CeO}_2\text{-TiO}_2$  surface, as demonstrated by the  $\text{H}_2$ -TPR technique. The SCR activity of  $\text{WO}_3\text{-CeO}_2\text{-TiO}_2$  system is higher than that of  $\text{CeO}_2\text{-TiO}_2$  in the whole temperature range. Hence, the NO conversion increases over the catalyst containing 10 %  $\text{WO}_3$  from 10 % (at 197 °C) to 90 % (at 320 °C) and remains above 90 % between 320 and 430 °C. The superior catalytic performance of this sample if compared to that prepared without tungsten can be principally correlated, according to the  $\text{H}_2$ -TPR results, with the presence of more reactive surface oxygen and redox sites due to the existence of  $\text{W}\leftrightarrow\text{Ce}$  interactions as previously explained [26]. It should be mentioned that the decrease of the NO conversion at high temperature (particularly for  $T > 400$  °C) over  $\text{CeO}_2\text{-TiO}_2$  and  $\text{WO}_3\text{-CeO}_2\text{-TiO}_2$  catalysts is due to the secondary reaction of  $\text{NH}_3$  oxidation [41]. In fact, figure 6B clearly shows that for these two samples,  $\text{NH}_3$  conversion reaches 100 % at 375 °C and remains at this value up to 500 °C. This means that from around 330 °C, more ammonia is consumed than NO. Therefore,  $\text{NH}_3$  conversion due to direct oxidation by  $\text{O}_2$  was also reported in Fig 6B. This conversion was inferred from the difference between the total  $\text{NH}_3$  conversion and the  $\text{NH}_3$  conversion involved in NO reduction. This side reaction starts around 320-330 °C for  $\text{CeO}_2\text{-TiO}_2$  and  $\text{WO}_3\text{-CeO}_2\text{-TiO}_2$  catalysts and becomes important above 400 °C.

The addition of sulfate groups into  $\text{CeO}_2\text{-TiO}_2$  had a different effect than that observed with tungsten species. It induces a visible decrease of the NO conversion at low temperature ( $< 300$  °C) but it increases significantly this conversion into  $\text{N}_2$  at high temperatures ( $> 300$  °C). Hence, the sulfated sample was found inactive until 300 °C after which the NO conversion increases with the increase of the reaction temperature up to 500 °C. Above 90 % NO conversions are reached over this sample in the 450-500 °C temperature range. For this catalyst, contrarily to  $\text{CeO}_2\text{-TiO}_2$  and  $\text{WO}_3\text{-CeO}_2\text{-TiO}_2$  solids, we observe a quite similar conversion of NO and  $\text{NH}_3$  (Fig. 6B) since direct  $\text{NH}_3$  oxidation by  $\text{O}_2$  is insignificant. Based

on this result, it can be confirmed, in line with the UV-vis results, that the presence of sulfate groups modifies the nature of cerium species suppressing the active ones for the low temperature  $\text{NH}_3$ -SCR reaction. By contrast, it induces, as shown by  $\text{NH}_3$ -TPD analysis, the formation of highly active acid sites for the high temperature NO reduction ( $> 450^\circ\text{C}$ ).

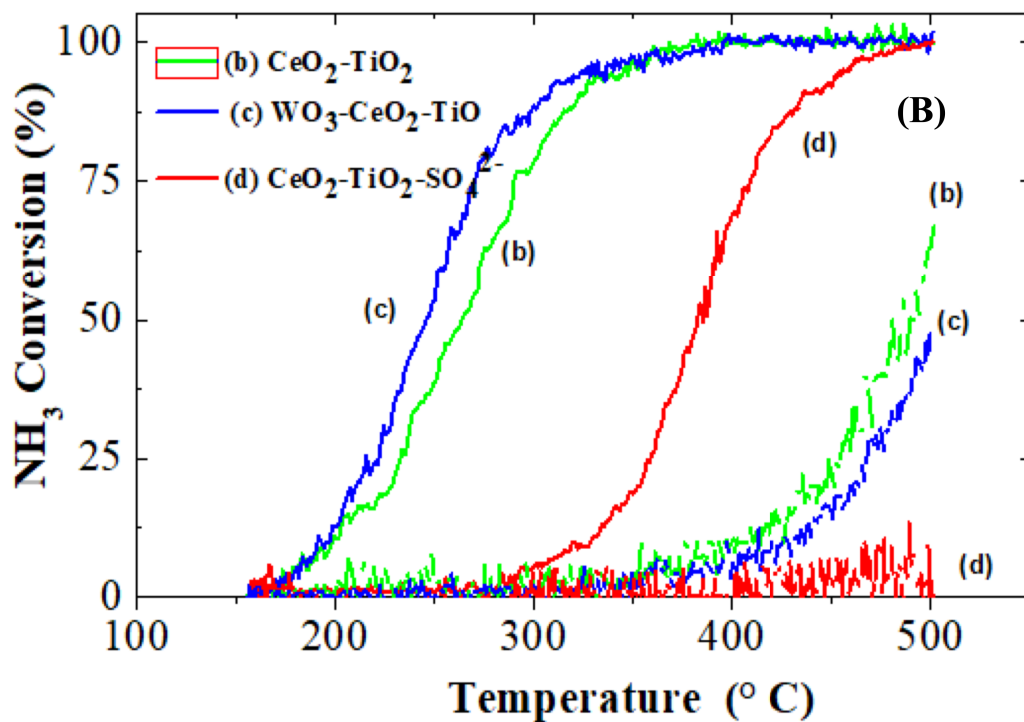
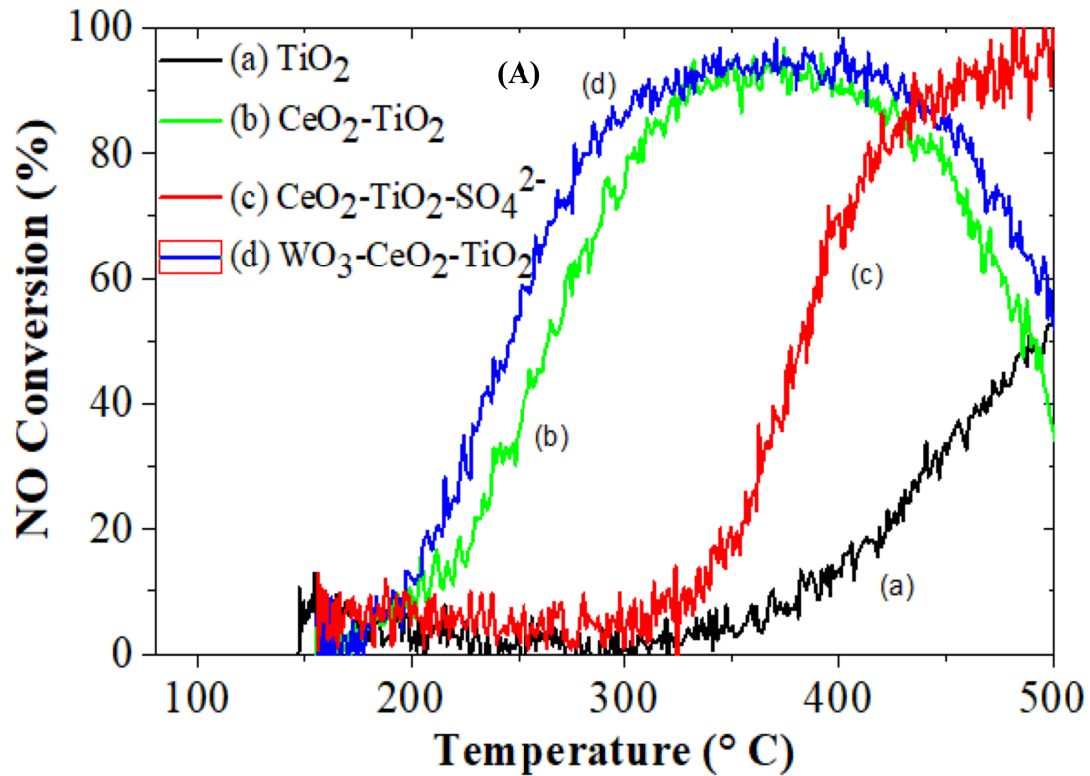


**Figure 6.** NH<sub>3</sub>-SCR performances of Ce based nanoporous aerogel catalysts: **(A)** NO conversion, **(B)** Total conversion (—) and Oxidation conversion (...) of NH<sub>3</sub>. Reaction conditions: [NO] = [NH<sub>3</sub>] = 0.04 %; [O<sub>2</sub>] = 8.00 %; He as balance; (GHSV) = 120 000 h<sup>-1</sup>.

## Conclusion

A comparative investigation about the effect of acidic components (SO<sub>4</sub><sup>2-</sup> and WO<sub>3</sub>) on the physico-chemical properties and NH<sub>3</sub>-SCR activity of CeO<sub>2</sub>-TiO<sub>2</sub> aerogel catalysts was reported for the first time in this study. The results revealed that the addition of sulfate groups obviously decreases the NO conversion at low temperature (< 300 °C), by changing the nature of Ce species, but it induces the formation of strong acid sites which were found highly active for the NO reduction into N<sub>2</sub> at high temperature (> 450 °C). The incorporation of WO<sub>3</sub> affects slightly the surface acidity of solid and contributes to the creation of more reactive surface oxygen and redox sites leading to more active catalyst at low temperature NH<sub>3</sub>-SCR (< 400 °C). The CeO<sub>2</sub>-TiO<sub>2</sub>-SO<sub>4</sub><sup>2-</sup>aerogel system exhibits, thanks to the high reactivity of acid sites generated by sulfate groups, the best SCR activity at high temperature. However, superior SCR performance was obtained at lower temperature (< 400 °C) over the WO<sub>3</sub>-CeO<sub>2</sub>-TiO<sub>2</sub> system due to the good reactivity of its redox sites and high concentration of surface oxygen.

## Declarations:

**Ethics approval and consent to participate:** Not applicable

**Consent for publication:** Not applicable

**Availability of data and materials:** Not applicable

**Competing interests:** There are no conflicts of interest to declare

**Funding:** Not applicable

**Authors contributions:** **Jihene Arfaoui:** Conceptualization, Methodology, Validation, Formal analysis, Investigation, Writing – original draft, writing-original draft preparation, Writing – review & editing, Supervision, Project administration, Funding acquisition, Resources. **Abdelhamid Ghorbel:** Methodology, Validation, Resources, Writing – review & editing, Project administration, Funding acquisition. **Carolina Petitto:** Methodology, Formal analysis, Investigation. **Gerard Delahay:** Methodology, Validation, Resources, Writing – review & editing, Funding acquisition. All authors have read and agreed to the published version of the manuscript.

### **Acknowledgements**

We gratefully acknowledge Thomas Cacciaguerra for XRD analysis. FrancoTunisian Cooperation (French Institute of Tunisia, SSHN grant) and Laboratory of Chemistry of Materials and Catalysis (LCMC) of Tunisia are gratefully acknowledged for the financial support.

### **References**

- [1] I. A. Resitoglu, K. Altinisik, A. Keskin, The pollutant emissions from diesel-engine vehicles and exhaust aftertreatment systems. *Clean Techn Environ Policy* 17 (2015) 15-27
- [2] F. Gholami, M. Tomas, Z. Gholami, M. Vakili, Technologies for the nitrogen oxides reduction from flue gas: A review. *Sci Total Environ* 714 (2020) 136712
- [3] C. Liu, J. W. Shi, C. Gao, C. Niu, Manganese oxide-based catalysts for low-temperature selective catalytic reduction of NO<sub>x</sub> with NH<sub>3</sub>: A review. *Appl Catal A: Gen* 522 (2016) 54-69
- [4] W. Shan, Y. Geng, Y. Zhang, Z. Lian, H. He, A CeO<sub>2</sub>/ZrO<sub>2</sub>-TiO<sub>2</sub> Catalyst for the Selective Catalytic Reduction of NO<sub>x</sub> with NH<sub>3</sub>. *Catalysts* 8 (2018) 592

- [5] F. Gao, X. Tang, H. Yi, S. Zhao, L. Chen, J. Li, Y. Shi, X. Meng, A Review on Selective Catalytic Reduction of NO<sub>x</sub> by NH<sub>3</sub> over Mn-Based Catalysts at Low Temperatures: Catalysts, Mechanisms, Kinetics and DFT Calculations. *Catalysts* 7 (2017) 199
- [6] B. Giechaskiel, R. Suarez-Bertoa, T. Lähde, M. Clairotte, M. Carriero, P. Bonnel, M. Maggiore, Evaluation of NO<sub>x</sub> emissions of a retrofitted euro 5 passenger car for the horizon prize “engine retrofit”. *Environ Res* 166 (2018) 298–309
- [7] L. Han, S. Cai, M. Gao, J. Y. Hasegawa, P. Wang, J. Zhang, L. Shi, D. Zhang, Selective Catalytic Reduction of NO<sub>x</sub> with NH<sub>3</sub> by Using Novel Catalysts: State of the Art and Future Prospects. *Chem Rev.* 119 (2019) 10916-10976
- [8] C. Chen, Y. Cao, S. Liu, J. Chen, W. Jia, Review on the latest developments in modified vanadium-titanium-based SCR catalysts. *Chinese J. Catal.* 39 (2018) 1347-1365
- [9] H. Wang, B. Huang, C. Yu, M. Lu, H. Huang, Y. Zhou, Research progress, challenges and perspectives on the sulfur and water resistance of catalysts for low temperature selective catalytic reduction of NO<sub>x</sub> by NH<sub>3</sub>. *Appl. Catal. A Gen:* 588 (2019) 217207
- [10] P. Granger, V. I. Parvulescu, Catalytic NO<sub>x</sub> abatement systems for mobile sources: From three-way to lean burn after-treatment technologies. *Chem. Rev.* 111 (2011) 3155-3207
- [11] Y. Peng, J. H. Li, X. Huang, X. Li, W. K. Su, X. Sun, D. Z. Wang, J. Hao Deactivation mechanism of potassium on the V<sub>2</sub>O<sub>5</sub>/CeO<sub>2</sub> catalysts for SCR reaction: acidity, reducibility and adsorbed-NO<sub>x</sub>. *Environ. Sci. Technol.* 48 (2014) 4515–4520
- [12] G. Busca, L. Lietti, G. Ramis, F. Berti Chemical and mechanistic aspects of the selective catalytic reduction of NO<sub>x</sub> by ammonia over oxide catalysts: A review. *Appl Catal B* 18 (1998) 1-36
- [13] L. Pang, C. Fan, L. Shao, J. Yi, X. Cai, J. Wang, M. Kang, T. Li, Effect of V<sub>2</sub>O<sub>5</sub>/WO<sub>3</sub>-TiO<sub>2</sub> catalyst preparation method on NO<sub>x</sub> removal from diesel exhaust, *Chinese J. Catal.* 35 (2014) 2020–2028

- [14] W. Shan, F. Liu, H. He, X. Shi, C. Zhang, A superior Ce-W-Ti mixed oxide catalyst for the selective catalytic reduction of NO<sub>x</sub> with NH<sub>3</sub>, *Appl. Catal. B: Environ.* 115-116 (2012) 100-106.
- [15] Z. Song, P. Ning, Q. Zhang, H. Li, J. Zhang, Y. Wang, X. Liu, Z. Huang, Activity and hydrothermal stability of CeO<sub>2</sub>-ZrO<sub>2</sub>-WO<sub>3</sub> for the selective catalytic reduction of NO<sub>x</sub> with NH<sub>3</sub>. *J. Environ. Sci.* 42 (2016)168-177.
- [16] Y. Zeng, K. G. Haw, Y. Wang, S. Zhang, Z. Wang, Q. Zhong, S. Kawi, Recent Progress of CeO<sub>2</sub>-TiO<sub>2</sub> Based Catalysts for Selective Catalytic Reduction of NO<sub>x</sub> by NH<sub>3</sub>. *ChemCatalChem* (2020) <http://dx.doi.org/10.1002/cctc.202001307>
- [17] P. Forzatti, Present status and perspectives in de-NO<sub>x</sub> SCR catalysis. *Appl. Catal. A Gen:* 222 (2001)221-236
- [18] T. Grzybek, Layered clays as SCR deNO<sub>x</sub> catalysts. *Catal. Today*, 119 (2007) 125-132
- [19] W. Shan, Y. Yu, Y. Zhang, G. He, Y. Peng, J. Li, H. He, Theory and practice of metal oxide catalyst design for the selective catalytic reduction of NO<sub>x</sub> with NH<sub>3</sub>. *Catal. Today* (2020) <https://doi.org/10.1016/j.cattod.2020.05.015>.
- [20] J. Arfaoui, A. Ghorbel, C. Petitto, G. Delahay, Novel V<sub>2</sub>O<sub>5</sub>-CeO<sub>2</sub>-TiO<sub>2</sub>-SO<sub>4</sub><sup>2-</sup> nanostructured aerogel catalyst for the low temperature selective catalytic reduction of NO by NH<sub>3</sub> in excess O<sub>2</sub>. *Appl Catal B: Environ* 224 (2018) 264-275
- [21] W. Shan, F. Liu, Y. Yu, H. He, The use of ceria for the selective catalytic reduction of NO<sub>x</sub> with NH<sub>3</sub>. *Chin J Catal* 35 (2014) 1251-1259
- [22] X. Gao, Y. Jiang, Y. Zhong, Z. Y. Luo, K. F. Cen, The activity and characterization of CeO<sub>2</sub>/TiO<sub>2</sub> catalysts prepared by sol gel method for selective catalytic reduction of NO with NH<sub>3</sub>. *J. Hazard. Mater.* 2010, 174, 734-739.

- [23] X. Gao, Y. Jiang, Y. C. Fu, Y. Zhong, Z. Y. Luo, K. F. Cen, Preparation and characterization of CeO<sub>2</sub>/TiO<sub>2</sub> catalysts for selective catalytic reduction of NO with NH<sub>3</sub>, Catal. Commun. 2010, 11, 465-469
- [24] H. Chang, L. Ma, S. Yang, J. Li, L. Chen, W. Wang, J. Hao, Comparison of preparation methods for ceria catalyst and the effect of surface and bulk sulfates on its activity toward NH<sub>3</sub>-SCR. J Hazard Mater 262 (2013) 782-788
- [25] F. Li, Y. Zhang, D. Xiao, D. Wang, X. Pan, X. Yang, Hydrothermal method prepared Ce-P-O catalyst for the selective catalytic reduction of NO with NH<sub>3</sub> in a broad temperature range. ChemCatChem 2 (2010) 1416-1419.
- [26] J. Arfaoui, A. Ghorbel, C. Petitto, G. Delahay, New CeO<sub>2</sub>-TiO<sub>2</sub>, WO<sub>3</sub>-TiO<sub>2</sub> and WO<sub>3</sub>-CeO<sub>2</sub>-TiO<sub>2</sub> mesoporous aerogel catalysts for the low temperature selective catalytic reduction of NO by NH<sub>3</sub>. J. Porous. Mater. (2021) <https://doi.org/10.1007/s10934-021-01102-3>
- [27] Y. Jiang, Z. Xing, X. Wang, S. Huang, Q. Liu, J. Yang, MoO<sub>3</sub> modified CeO<sub>2</sub>/TiO<sub>2</sub> catalyst prepared by a single step sol-gel method for selective catalytic reduction of NO with NH<sub>3</sub>, J Ind Eng Chem 29 (2015) 43-47
- [28] Y. Jiang, C. Bao, S. Liu, G. Liang, M. Lu, C. Lai, W. Shi, S. Ma, Enhanced Activity of Nb-modified CeO<sub>2</sub>/TiO<sub>2</sub> Catalyst for the Selective Catalytic Reduction of NO with NH<sub>3</sub>. Aerosol Air Qual Res 18 (2018) 2121-2130
- [29] Y. Yu, J. Zhang, C. Chen, M. Ma, C. He, J. Miao, H. Li, J. Chen, Selective catalytic reduction of NO with NH<sub>3</sub> over TiO<sub>2</sub> supported metal sulfate catalysts prepared via a sol-gel protocol. New J Chem 44 (2020) 13598-13605
- [30] L. Li, W. Tan, X. Wei, Z. Fan, A. Liu, K. Guo, K. Ma, S. Yu, C. Ge, C. Tang, L. Dong, Mo doping as an effective strategy to boost low temperature NH<sub>3</sub>-SCR performance of CeO<sub>2</sub>/TiO<sub>2</sub> catalysts. Catal Comm 114 (2018) 10-14

- [31] H. Jensen, A. Soloviev, Z. Li, E. G. Søgaard, XPS and FTIR investigation of the surface properties of different prepared titania nano-powders, *Appl. Surf. Sci.* 246 (2005)239-249.
- [32] H. Maleki, Recent Advances in Aerogels for Environmental Remediation Applications, *Chem. Eng. J.* 300 (2016) 98-118.
- [33] K. Cheng, J. Liu, T. Zhang, J. Li, Z. Zhao, Y. Wei, G. Jiang, A Duan Effect of Ce doping of TiO<sub>2</sub> support on NH<sub>3</sub>-SCR activity over V<sub>2</sub>O<sub>5</sub>-WO<sub>3</sub>/CeO<sub>2</sub>-TiO<sub>2</sub> catalyst. *J Environ Sci* 26 (2014) 2106-2113.
- [34] J. Arfaoui, A. Ghorbel, C. Petitto, G. Delahay, Promotional effect of ceria on the catalytic behaviour of V<sub>2</sub>O<sub>5</sub>-WO<sub>3</sub>-TiO<sub>2</sub> aerogel solids for the DeNO<sub>x</sub> process. *J. Solid. State Chem.* 300: (2021) 122261
- [35] L. Chen, D. Weng, Z. Si, X. Wu, Synergistic effect between ceria and tungsten oxide on WO<sub>3</sub>-CeO<sub>2</sub>-TiO<sub>2</sub> catalysts for NH<sub>3</sub>-SCR reaction. *Prog Nat Sci* 22 (2012) 265-272.
- [36] X. Du, X. Wang, Y. Chen, X. Gao, L. Zhan, Supported metal sulfates on Ce-TiO<sub>x</sub> SCR as catalysts for NH<sub>3</sub>-SCR of NO: High resistances to SO<sub>2</sub> and potassium. *J. Ind. Eng. Chem.* 36 (2016) 271-278
- [37] W. Shan, F. Liu, H. He, X. Shi, C. Zhang, An environmentally-benign CeO<sub>2</sub>-TiO<sub>2</sub> catalyst for the selective catalytic reduction of NO<sub>x</sub> with NH<sub>3</sub> in simulated diesel exhaust. *Catal Today* 184 (2012) 160-165
- [38] M. Thommes, K. Kaneko, A. V. Neimark, J. P. Olivier, F. Rodriguez-Reinoso, J. Rouquerol, K. S. W. Sing, Physisorption of gases, with special reference to the evaluation of surface area and pore size distribution (IUPAC Technical Report). *Pure Appl Chem* 87 (2015) 1051-1069
- [39] G. Imran, R. Maheswari, Mn-incorporated SBA-1 cubic mesoporous silicates: Synthesis and characterization. *Mater Chem Phys* 161(2015) 237-242

- [40] M. A. López-Mendoza, R. Nava, C. Peza-Ledesma, B. Millán-Malo, R. Huirache-Acuña, P. Skewes, E. M. Rivera-Muñoz, Characterization and catalytic performance of Co-Mo-W sulfide catalysts supported on SBA-15 and SBA-16 mechanically mixed. *Catal Today* 271 (2016) 114-126
- [41] Arfaoui J, Ghorbel A, Petitto C, Delahay G, A new  $V_2O_5$ - $MoO_3$ - $TiO_2$ - $SO_4^{2-}$  nanostructured aerogel catalyst for Diesel DeNOx technology. *New J. Chem.* 44, (2020) 16119-16134.
- [42] H. Chen, Y. Xia, H. Huang, Y. Gan, X. Tao, C. Liang, J. Luo, R. Fang, J. Zhang, W. Zhang, X. Liu, Highly dispersed surface active species of Mn/Ce/TiW catalysts for high performance at low temperature  $NH_3$ -SCR. *Chem. Eng. J.* 330 (2017) 1195–1202.
- [43] M. A. Larrubia, G. Busca, An ultraviolet-visible-near infrared study of the electronic structure of oxide supported vanadia tungsta and vanadia molybdena. *Mater Chem Phys* 72 (2001) 337–436.
- [44] J. Arfaoui, A. Ghorbel, C. Petitto, G. Delahay, New  $MoO_3$ - $CeO_2$ - $ZrO_2$  and  $WO_3$ - $CeO_2$ - $ZrO_2$  nanostructured mesoporous aerogel catalysts for the  $NH_3$ -SCR of NO from diesel engine exhaust. *J. Ind. Eng. Chem.* 95 (2021) 182-189
- [45] W. J. Roth, B. Gil, W. Makowski, A. Sławek, A. Korzeniowska, J. Grzybek, M. Siwek, P. Michorczyk, Framework-substituted cerium MCM-22 zeolite and its interlayer expanded derivative MWW-IEZ, *Catal Sci Technol* (2016) <http://dx.doi.org/10.1039/c5cy02074c>
- [46] Y. Shao, L. Wang, J. Zhang, M. Anpo, Synthesis of hydrothermally stable and longrange ordered Ce-MCM-48 and Fe-MCM-48 materials. *J Phys Chem B* 109 (2005) 20835–20841
- [47] J Arfaoui, A Ghorbel, C Petitto, G Delahay New Mn- $TiO_2$  aerogel catalysts for the low temperature Selective Catalytic Reduction of NOx. *J. Sol-Gel Sci. Technol.* 97 (2021) 302–310

- [48] J. Du, X. Shi, Y. Shan, G. Xu, Y. Sun, Y. Wang, Y. Yu, W. Shan, H. He, Effects of SO<sub>2</sub> on Cu-SSZ-39 catalyst for the selective catalytic reduction of NO<sub>x</sub> with NH<sub>3</sub>. *Catal Sci Technol* 10 (2020) 1256-1263
- [49] X. Huang, Z. Liu, D. Wang, Y. Peng, J. Li, The effect of additives and intermediates on vanadia-based catalyst for multi-pollutant control. *Catal Sci Technol* 10 (2020) 323- 326
- [50] Z. Song, Y. Xing, T. Zhang, J. Zhao, J. Wang, Y. Mao, B. Zhao, X. Zhang, M. Zhao, Z. Ma, Effectively promoted catalytic activity by adjusting calcination temperature of Ce-Fe-Ox catalyst for NH<sub>3</sub>-SCR. *Appl Organometal Chem* e5446 (2019) <https://doi.org/10.1002/aoc.5446>
- [51] Y. Ke, W. Huang, S. Li, Y. Liao, J. Li, Z. Qu, N. Yan, Surface acidity enhancement of CeO<sub>2</sub> catalysts via modification with a heteropoly acid for the selective catalytic reduction of NO with ammonia. *Catal Sci Technol* 9 (2019) 5774-5785
- [52] C. Gannoun, R. Delaigle, P. Eloy, D. P. Debecker, A. Ghorbel, E. M. Gaigneaux, Effect of support on V<sub>2</sub>O<sub>5</sub> catalytic activity in chlorobenzene oxidation. *Appl Catal A* 1-6 (2012) 447–448
- [53] L. Lietti, J. L. Alemany, P. Forzatti, G. Busca, G. Ramis, E. Giamello and F. Bregani, Reactivity of V<sub>2</sub>O<sub>5</sub>–WO<sub>3</sub>/TiO<sub>2</sub> catalysts in the selective catalytic reduction of nitric oxide by ammonia, *Catal. Today*, 1996, 29, 143–148